

Coexistence of magnetism and superconductivity: Tunneling characteristics of magnetic superconductors

M. J. Nass and K. Levin

*The James Franck Institute and The Department of Physics,
University of Chicago, Chicago, Illinois 60637*

G. S. Grest

Department of Physics, Purdue University, West Lafayette, Indiana 47907

(Received 13 May 1980)

We compute the superconducting density of states $N_s(\omega)$ for a magnetically ordered superconductor. In principle, $N_s(\omega)$ contains valuable information about the magnetic correlations. To illustrate how to extract this information, we numerically solve the full (Eliashberg-like) integral equation for $N_s(\omega)$. This depends on the magnetic structure factor $S(q, \omega)$. Our results are compared with tunneling measurements on a (proximity-effect-) induced superconducting spin-glass. In general, we find good agreement with experiment for the temperature dependence of the zero-bias conductance for two different models of $S(q, \omega)$ in a spin-glass. These models, which are constrained to satisfy sum rules, are compared with direct neutron measurements. A calculation of the gap (Δ)-dependent spin-exchange lifetime $1/\tau_s^{\text{eff}} \equiv \Delta \{ 1 - [N_s(0)/N(0)]^2 \}^{-1/2}$ is found to yield significantly better agreement with experiment than the usual golden rule calculation (which includes inelastic processes). For the spin-glasses our theory predicts a temperature-dependent peak in $dN_s(\omega)/d\omega$ at $\omega \sim T_{\text{sg}}$, where T_{sg} is the transition temperature. To observe this feature and others, we urge that further measurements of the tunneling characteristics of intrinsic magnetic superconductors be performed.

I. INTRODUCTION

Recent observations of magnetic and superconducting order in the ternary rare-earth borides and chevelon compounds^{1,2} and induced spin-glass superconductivity³ have reopened interest in the problem of coexistent order. In those materials and in alloys containing magnetic impurities the Cooper paired electrons are strongly affected by the presence of magnetic ordering of the localized spins. Two distinct kinds of depairing effects can occur: (i) The magnetic component may introduce macroscopic internal magnetic fields which inhibit superconductivity. (ii) The superconducting electrons are "spin-flip" scattered as a result of their exchange interactions with the localized spins. In dilute alloys this effect can be parametrized by the spin-flip lifetime τ_s . For the nondilute case it is not generally possible to characterize simply these scattering effects. Rather, they must be included dynamically [through the magnetic structure factor $S(q, \omega)$] in the solution of the self-consistent Eliashberg equations for the transition temperature and superconducting density of states.

A measurement of the latter affords a convenient opportunity to study pair breaking due to scattering from localized spins. Furthermore, it gives an indication of whether coexistent order does, in fact, exist.

In principle, it also yields information about the magnetic structure factor $S(q, \omega)$: tunneling measurements can be exploited (in much the same way as done by McMillan and Rowell⁴ for the phonon case) to learn about the details of the spin-spin correlations in magnetic superconductors.

It is the purpose of the present paper to compute the superconducting density of states for a (nondilute) magnetic superconductor. We thus derive a dynamical generalization of the spin-flip scattering time. Our aims are the following:

(i) To show how to incorporate spin-flip scattering into the superconducting gap equations when the magnetic ions interact strongly with each other. We thus generalize and numerically solve the equivalent of the Abrikosov-Gor'kov equations⁵ in the nondilute limit.

(ii) To predict features in the superconducting density of states (as measured in tunneling experiments).

(iii) To interpret recent tunneling experiments³ in induced-spin-glass superconductors and from these to gain information about $S(q, \omega)$ in these materials.

While we will not discuss details of the phase diagram for magnetic and superconducting order, our results bear directly on this problem. In the interesting case, when superconducting and magnetic order coexist, it is clear that the "bare" transition tempera-

tures must be comparable in magnitude. In this limit the dynamics of the magnetic spin-superconducting electron interaction must be fully included, as we do here.

Theoretical studies of the effects of magnetic interactions on superconducting order are numerous.⁵⁻¹⁴ Our work may be compared to that of Keller and Benda.⁷ These authors considered dynamical effects in their general expressions for the self-energies, but did not include them in solving these equations. Similarly, Maekawa and Tachiki¹⁰ included inelastic processes in their formalism, but used a weak-coupling approximation to solve for the transition temperature T_c . Their work is similar in spirit to that of Berk and Schrieffer¹⁵ who studied the effect of paramagnons on T_c . By contrast in our numerical work we use the full $S(q, \omega)$. Furthermore we focus on the superconducting density of states rather than the magnetic-superconducting phase diagram and we, unlike many others, include the possibility of magnetic order (of a general nature) in our formal equations as well as in their specific numerical solution.

The effects of spatial (rather than dynamical) correlations on the spin-flip scattering time have been dealt with exhaustively.¹⁶ Those calculations are generally appropriate to the case in which there is no magnetic order in the superconducting phase.

Because we are concerned with tunneling experiments on induced superconductors, our work may be compared with that of Kaiser and Zukerman.¹⁷ These authors considered the case of noninteracting magnetic impurities. However, they solved for the (proximity-effect-) induced superconducting density of states self-consistently, following McMillan.¹⁸ To generalize their work to the case of interacting spins is difficult, since it involves the solution of two coupled integral equations, corresponding to the normal (N) and superconducting (S) pieces of the sandwich. Therefore, in our discussion of proximity-effect-induced superconductivity, we will treat the tunnel junction only approximately. The S piece is included only insofar as it gives rise to a gap function Δ in the induced superconductor (N piece).

The remainder of the paper is divided into three sections. In Sec. II we present a calculation of the general expression for the superconducting density of states $N_s(\omega)$ for the case of a superconductor containing interacting magnetic spins (which may or may not be ordered). The actual computation of $N_s(\omega)$ involves the solution of an Eliashberg-like integral equation which is a function of the magnetic structure factor $S(q, \omega)$. We solve this equation numerically in Sec. III. Using two different models for $S(q, \omega)$ we consider the specific case of a superconducting spin-glass. For this case, our results can be directly compared with experiment. In Sec. III A we discuss these two models in some detail. In Sec. III B we present numerical results which are compared

with experiment for the temperature dependence of $N_s(0)$ and the ω and T dependence of $N_s(\omega)$. We plot and discuss the effective spin-flip, or spin-exchange scattering time and present theoretical predictions for the behavior of $dN_s/d\omega$ vs ω in superconducting spin-glasses. Finally in Sec. IV, we briefly summarize our conclusions.

II. GENERAL EXPRESSION FOR SUPERCONDUCTING DENSITY OF STATES

In this section we review a calculation of the superconducting density of states $N_s(\omega)$ for a superconductor containing localized spins. The spins are assumed to be sufficiently concentrated so that inter-spin interactions are non-negligible; these give rise indirectly to inelastic conduction-electron scattering processes.

The Hamiltonian for a system of electrons interacting with localized spins is given by

$$\mathcal{H} = \mathcal{H}^0 + \mathcal{H}^{\text{sd}} \quad (2.1)$$

where

$$\mathcal{H}^0 = \sum_k \epsilon(k) C_{k\sigma}^\dagger C_{k\sigma} + \sum_{kk'} V_{kk'} C_{k\uparrow}^\dagger C_{-k\downarrow}^\dagger C_{-k'\downarrow} C_{k'\uparrow} \quad (2.2)$$

and

$$\mathcal{H}^{\text{sd}} = \frac{1}{2} J^{\text{sd}} \sum_{ikk', \sigma\sigma'} \exp[i(\vec{k} - \vec{k}') \cdot \vec{R}_i] \times (\vec{S}_i \cdot C_{k\sigma}^\dagger \vec{\sigma}_{\sigma\sigma'} C_{k'\sigma'}) \quad (2.3)$$

Here $\vec{\sigma}_{\sigma\sigma'}$ is the vector Pauli matrix and J^{sd} [which is assumed independent of $(\vec{k} - \vec{k}')$, for simplicity] is the exchange interaction between the conduction electrons and localized spins. The electron phonon interaction, which is treated using the BCS (weak-coupling) model, gives rise to an effective electron-electron interaction $V_{kk'}$, and $\epsilon(k)$ is the electron kinetic energy.

It is convenient to rewrite \mathcal{H} by adding and subtracting the mean-field term associated with long-range unidirectional magnetic order

$$\mathcal{H}^{\text{mf}} = \sum_k H(G) (C_{K+G\uparrow}^\dagger C_{k\downarrow}^\dagger - C_{k+G\downarrow}^\dagger C_{K\uparrow}) \quad (2.4)$$

where $H(G) = M(G)J^{\text{sd}}$ is the molecular field deriving from the magnetic order parameter $M(G)$ and G is the magnetic lattice vector. This term when combined with the kinetic energy in Eq. (2.1) leads to a quasiparticle energy $E_\sigma(k)$, which will be discussed in detail in a future work.¹⁹ The Hamiltonian $\mathcal{H}^0 + \mathcal{H}^{\text{mf}}$ thus has associated with it a "bare" matrix Green's function

$$G_0^{-1}(\vec{k}, i\omega_n) = i\omega_n - \xi_{\sigma\rho_3} - \Delta_{\rho_2\sigma_2} \quad (2.5)$$

where $\xi_\sigma \equiv E_\sigma(k) - \mu$ and ω_n represents the Matsubara frequency. The matrices σ_i and ρ_i are the ordinary 2×2 (spinor) Pauli matrices acting in the spin and particle-hole space, respectively, of the electronic states. The Green's function of $\mathcal{H} = (\mathcal{H}^0 + \mathcal{H}^{\text{mf}}) + (\mathcal{H}^{\text{sd}} - \mathcal{H}^{\text{mf}})$ will be obtained using the self-consistent Hartree-Fock approximation. It is assumed to have the form

$$G^{-1}(\vec{k}, i\omega_n) = i\tilde{\omega}_n - \xi_\sigma \rho_3 - \tilde{\Delta} \rho_2 \sigma_2. \quad (2.6)$$

The two depairing effects of the localized spins, which were listed in Sec. I, enter into this description in distinct ways. The macroscopic magnetic fields enter through the quasiparticle energies $E_\sigma(k)$, whereas the spin-flip scattering gives rise to the difference between $G(k, i\omega_n)$ and $G_0(k, i\omega_n)$. Much

of the emphasis in the present paper is on the case of spin-glass superconductors for which molecular field effects can be ignored. This also pertains to the case of magnetic superconductors above the magnetic ordering temperatures. Additionally, to a reasonable approximation molecular field H_G effects may be ignored in antiferromagnetic superconductors since generally only a small fraction of the Fermi surface is affected by H_G . The interaction of the superconducting electrons with the spin fluctuations leads to a self-energy

$$\Sigma(\vec{k}, i\omega_n) \equiv G_0^{-1}(\vec{k}, i\omega_n) - G^{-1}(\vec{k}, i\omega_n), \quad (2.7)$$

which derives from the scattering term $(\mathcal{H}^{\text{sd}} - \mathcal{H}^{\text{mf}})$. An expression for $\Sigma(\vec{k}, \omega)$ can be obtained to order $(J^{\text{sd}})^2$

$$\Sigma(\vec{k}, i\omega_n) = -\frac{(J^{\text{sd}})^2}{\beta} \sum_m \int \frac{d^3k'}{(2\pi)^3} \tilde{\alpha} G(\vec{k}, i\omega_m) \cdot \tilde{\alpha} D(\vec{k} - \vec{k}', i(\omega_n - \omega_m)), \quad (2.8)$$

where $\tilde{\alpha} = \frac{1}{2}(1 + \rho_3)\tilde{\sigma} + \frac{1}{2}(1 - \rho_3)\sigma_2\tilde{\sigma}\sigma_2$. Here D is the time-ordered propagator for the localized spin. This has a spectral representation

$$D(q; i\omega_n) = \int_0^\infty d\Omega B(q, \Omega) \frac{2\Omega}{(i\omega_n)^2 - \Omega^2}, \quad (2.9)$$

where the spectral weight function $B(q, \Omega)$ is the Fourier transform of the commutator $i\Theta(t)\langle[S_i(t), S_j(0)]\rangle$ and i and j are site indices. Equating matrix elements, Eq. (2.8) can be rewritten

$$\omega_n - \tilde{\omega}_n = \frac{(J^{\text{sd}})^2}{\beta} \sum_m N(0) \int_0^{2k_F} \frac{q dq}{2k_F^2} \int_{-\infty}^\infty \frac{d\omega'}{(i\omega_n - \omega')} \text{Im} \left[\frac{\tilde{\omega}(\omega' + i\delta)}{[\tilde{\Delta}^2(\omega' + i\delta) - \tilde{\omega}^2(\omega' + i\delta)]^{1/2}} \right] D(\vec{q}; i(\omega_n - \omega_m)), \quad (2.10a)$$

$$\tilde{\Delta}_n - \Delta = \frac{(J^{\text{sd}})^2}{\beta} \sum_m N(0) \int_0^{2k_F} \frac{q dq}{2k_F^2} \int_{-\infty}^\infty \frac{d\omega'}{(i\omega_n - \omega')} \text{Im} \left[\frac{\tilde{\Delta}(\omega' + i\delta)}{[\tilde{\Delta}^2(\omega' + i\delta) - \tilde{\omega}^2(\omega' + i\delta)]^{1/2}} \right] D(\vec{q}; i(\omega_n - \omega_m)). \quad (2.10b)$$

In the above equations $(\omega' + i\delta)$ is an argument of the functions $\tilde{\Delta}$ and $\tilde{\omega}$, and we have used the spectral representation

$$G(i\omega_n) = \int_{-\infty}^\infty \frac{\text{Im}G(\omega' + i\delta)}{\omega' - i\omega_n} d\omega'. \quad (2.11)$$

Equations (2.10) have essentially been derived previously by Keller and Benda.⁷ They can be readily combined into one equation for

$$u(\omega) \equiv \tilde{\omega}(\omega)/\tilde{\Delta}(\omega), \quad (2.12)$$

which quantity is directly relevant for computing the density of states. Following Ref. 20 we may perform the summation over ω_m to obtain

$$u(\omega) = \frac{\omega}{\Delta} + \frac{N(0)}{\Delta} (J^{\text{sd}})^2 \int_0^{2k_F} \frac{q dq}{2k_F^2} \int_0^\infty d\Omega B(\vec{q}, \Omega) \times \int_{-\infty}^\infty d\omega' \left[\text{Im} \frac{u(\omega' + i\delta)}{[1 - u^2(\omega' + i\delta)]^{1/2}} + u(\omega) \text{Im} \frac{1}{[1 - u^2(\omega' + i\delta)]^{1/2}} \right] \times \left[\frac{f(-\omega') + n(\Omega)}{\omega' - \omega + \Omega} + \frac{f(\omega') + n(\Omega)}{\omega' - \omega - \Omega} \right], \quad (2.13)$$

where f and n are the usual Fermi and Bose occupation factors. Equation (2.13) is expressed as an integral over positive frequencies ω' by imposing the appropriate symmetry

$$u(-\omega) = -u^*(\omega).$$

This yields

$$\begin{aligned}
 u(\omega) = & \frac{\omega}{\Delta} + \frac{N(0)}{\Delta} (J^{\text{sd}})^2 \int_0^{2k_F} \frac{q \, dq}{2k_F^2} \int_0^\infty d\Omega B(\bar{q}, \Omega) \left[\pi n(\Omega) \left(\frac{u(\omega - \Omega) + u(\omega)}{[1 - u^2(\omega - \Omega)]^{1/2}} + \frac{u(\omega + \Omega) + u(\omega)}{[1 - u^2(\omega + \Omega)]^{1/2}} \right) \right. \\
 & + \int_0^\infty d\omega' \left(\text{Im} \frac{u(\omega')}{[1 - u^2(\omega')]^{1/2}} + u(\omega) \text{Im} \frac{1}{[1 - u^2(\omega')]^{1/2}} \right) \\
 & \times \left(\frac{f(-\omega')}{\omega' - \omega + \Omega} \mp \frac{f(-\omega')}{\omega' + \omega + \Omega} \right. \\
 & \left. \left. + \frac{f(\omega')}{\omega' - \omega - \Omega} \mp \frac{f(\omega')}{\omega' + \omega - \Omega} \right) \right] , \quad (2.14)
 \end{aligned}$$

where the upper and lower signs correspond to the first and second term in the preceding large parentheses. Here we have separated the Bose- and Fermi-like contributions for convenience. The sign conventions in Eq. (2.14) are such that $\text{Im}u(\omega + i\delta) > 0$ for all ω .

The density of states $N_s(\omega)$ is related to $u(\omega)$ by

$$N_s(\omega) = N(0) \text{Im} \left[\frac{u(\omega)}{[1 - u^2(\omega)]^{1/2}} \right] . \quad (2.15)$$

It should be noted that Eqs. (2.14) and (2.15) thus constitute a generalization of the Abrikosov-Gorkov⁵ (AG) equations for the case of interacting spins. In the noninteracting limit

$$B(q, \Omega) = \frac{1}{2} n S(S+1) (1 - e^{-\beta\Omega}) \delta(\Omega) .$$

We obtain the AG result directly from Eqs. (2.14) and (2.15)

$$N_s(\omega) = N(0) \zeta^{-1} \text{Im}u(\omega) , \quad (2.16)$$

where $\zeta^{-1} = \tau_s^\infty \Delta$ and $1/\tau_s^\infty$ is given by the golden rule approximation for elastic scattering processes

$$1/\tau_s^\infty = n \pi N(0) S(S+1) (J^{\text{sd}})^2 \quad (2.17)$$

and n is the concentration of impurities. Equation (2.14) makes it evident that structure in the spectral weight function $B(q, \Omega)$ is directly reflected in that of the superconducting density of states $N_s(\omega)$. This is similar to the case of strong-coupling superconductivity, in which case $B(q, \Omega)$ is the appropriate phonon spectral weight function.

While it may be generally difficult to separate the phonon- and spin-fluctuation induced structure in the tunneling characteristics, it seems possible, at least in principle, to achieve such a separation by looking at temperature-dependent effects or structure at low frequencies. Magnetic excitations (which, when coexistent order occurs, have low characteristic temperatures ~ 10 K) should lead to stronger temperature dependences in $N_s(\omega)$ than do the phonons. Furth-

ermore, the low frequency structure of the magnetic excitations often does not overlap that of the phonon frequencies.

The quantity $B(q, \omega)$ can be readily related to the static structure factor

$$\begin{aligned}
 B(q, \omega) = & \frac{1}{2} (1 - e^{-\beta\omega}) \\
 & \times [S(q, \omega) + \pi \langle \bar{S}(q) \rangle \cdot \langle \bar{S}(-q) \rangle \delta(\omega)] , \quad (2.18)
 \end{aligned}$$

where

$$\begin{aligned}
 S(q, \omega) = & \int_{-\infty}^\infty dt [\langle \bar{S}(q, t) \cdot \bar{S}(-q, 0) \rangle \\
 & - \langle \bar{S}(q) \rangle \cdot \langle \bar{S}(-q) \rangle] e^{i\omega t} . \quad (2.19)
 \end{aligned}$$

It should be noted that in our definition of $B(q, \omega)$ we have kept track explicitly of the "elastic" term proportional to $\omega\delta(\omega)$ since it leads to a finite (elastic) contribution to $u(\omega)$ in the integral equation. So far our results have been general and apply to all types of magnetic order: unidirectional ferro- and antiferromagnets as well as spin-glasses. For the first case, the magnetic sublattice vector $G = 0$ whereas for the latter $G \neq 0$. For the spin-glass case we can ignore the addition and subtraction of \mathcal{J}^{mf} which was described above. This follows because there is no long-range or periodic order. For a random system the structure factor in Eq. (2.18) becomes

$$\begin{aligned}
 S(q, \omega) = & \int_{-\infty}^\infty dt \{ [\langle \bar{S}(q, t) \cdot \bar{S}(-q, 0) \rangle]_c \\
 & - [\langle \bar{S}(q) \rangle]_c [\langle \bar{S}(-q) \rangle]_c \} e^{i\omega t} , \quad (2.20)
 \end{aligned}$$

where $[\]_c$ denotes a configuration average. It should be noted that a consequence of this definition is that in a spin-glass $S(q, \omega)$ contains a term proportional to $\delta(\omega)$. The subtracted term in Eq. (2.20) is chosen so that $\mathcal{J}^{\text{sd}} - \mathcal{J}^{\text{mf}}$ describe scattering relative to the *periodic* background potential.¹⁹ In the spin-glass case this background is zero.

So far we have not discussed the quantity Δ . For intrinsic magnetic superconductors this has to be determined self-consistently by solving Eq. (2.14) to-

gether with the equation

$$\Delta = VN(0) \int_0^{\omega_c} d\omega' \operatorname{Im} \left(\frac{1}{[1 - u^2(\omega')]^{1/2}} \right) \tanh \frac{1}{2} \beta \omega' \quad (2.21)$$

Here $V_{kk'} = V\Theta(|\epsilon(k) - \mu| - \omega_c)\Theta(|\epsilon(k') - \mu| - \omega_c)$ and ω_c is the BCS cutoff frequency of the phonons. For proximity-effect-induced magnetic superconductors we will treat Δ as a phenomenological parameter whose magnitude is given by experiment. For the cases of specific interest it may be assumed that Δ is temperature independent.

III. APPLICATION TO TUNNELING EXPERIMENTS IN SPIN-GLASSES

There are, at present, apparently no tunneling measurements on intrinsic magnetic superconductors in the coexistent state. Such experiments appear to be feasible. In principle, they would yield interesting information about the interplay of magnetic and superconducting order. However, there do exist measurements of tunneling characteristics in (induced) superconducting spin-glasses.³ Therefore, for the remainder of this paper we shall focus on these materials.

In order to apply Eq. (2.14) one has to choose a model for the spectral weight function $B(q, \omega)$, or equivalently $S(q, \omega)$. This is discussed in Sec. III A.

A. Models for $S(q, \omega)$ in spin-glasses

In the Edwards-Anderson (EA) model²¹ the spectral weight function $B(q, \omega)$ (which is q independent) may be readily evaluated.²² This quantity is related to the magnetic structure factor as

$B(q, \omega) = \frac{1}{2}(1 - e^{-\beta\omega})S(q, \omega)$. We have

$$B(q, \omega) = \frac{1}{\sqrt{2\pi}} \int_0^\infty dr r^2 e^{-r^2/2} Z^{-1}(r) \times \sum_{mn} e^{-\beta E_n} (1 - e^{-\beta\omega}) \bar{S}_{nm} \cdot \bar{S}_{mn} \times \delta(\omega - E_m + E_n) \quad (3.1)$$

where

$$E_n = S_{nn}^z \bar{J} \left(\frac{1}{3} Q \right)^{1/2} r$$

and

$$Z(r) \equiv \sum_n \exp[-\beta S_{nn}^z \bar{J} \left(\frac{1}{3} Q \right)^{1/2} r]$$

Here the energies E_n and state $|n\rangle$ correspond to the eigenvalues and eigenfunctions of the mean-field Hamiltonian

$$\mathcal{H}(r) = \bar{J} \left(\frac{1}{3} Q \right)^{1/2} \bar{S}_i \quad (3.2)$$

and $Q = [\langle S_i^2 \rangle]_c$ is the EA order parameter and \bar{J} is the width of the Gaussian distribution of exchange interactions. Below the spin-glass transition temperature T_{sg} , $B(q, \omega)$ has a Gaussian width $e^{-\omega^2 \lambda}$ where $\lambda \propto 1/Q$. Above T_c , $B(q, \omega)$ is proportional to $\delta(\omega)$. These results may be readily generalized to include cluster spins,²² in which limit $B(q, \omega)$ is no longer q independent. A plot of $S(q, \omega)$ for spin $\frac{5}{2}$ derived from $B(q, \omega)$ [see Eq. (2.18)] is shown in Fig. 1 for several values of temperature T labeled a-d. For the EA model, Eq. (2.19), includes an elastic [$\propto \delta(\omega)$] contribution to $S(q, \omega)$, as noted above. The only free parameter in the EA model is \bar{J} , which we examined for the values $\frac{1}{12} \leq \bar{J}/\Delta \leq 2$. Here Δ is the superconducting gap parameter. It may be seen that $S(q, \omega)$ vanishes at $\omega = 0$ [except for the $\delta(\omega)$ term]. This derives from the factor d^3r in the integrand in Eq. (3.1). Thus the distribution of molecular fields $\mathcal{O}(H) d^3H$, where $H = \bar{J} \left(\frac{1}{3} Q \right)^{1/2} r$, has no contributing weight at the origin $H = r = 0$. While this is clearly inconsistent with experiment (see Fig. 2), it should be noted that in all relevant scattering processes there is an inelastic contribution as well as an elastic one [proportional to $\delta(\omega)$]. Since the separation between true elastic and quasielastic processes is difficult to achieve experimentally, this division is somewhat arbitrary. Thus it is probably not particularly significant that the EA model tends to make this separation differently than does experiment. We expect that all calculations based on this dynamical model which depend on frequency integrals of $S(q, \omega)$ are therefore not unreasonable.

The overall width of $S(q, \omega)$ is of the order of $k_B T_{\text{sg}}$ at low T and decreases to zero at and above T_{sg} . This critical narrowing will not occur when spin clusters are included. Furthermore it is not observed experimentally²³ as may be seen from the neutron data which is reproduced in Fig. 2.

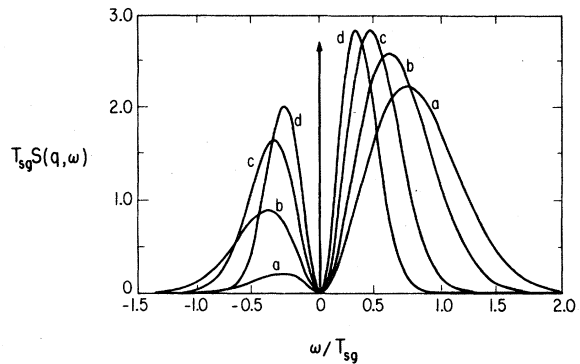


FIG. 1. Magnetic structure factor for the Edwards-Anderson (EA) mean-field model with $S = \frac{5}{2}$ at temperatures a $T/T_{\text{sg}} = 0.2$; b $T/T_{\text{sg}} = 0.4$; c $T/T_{\text{sg}} = 0.7$; and d $T/T_{\text{sg}} = 0.9$.

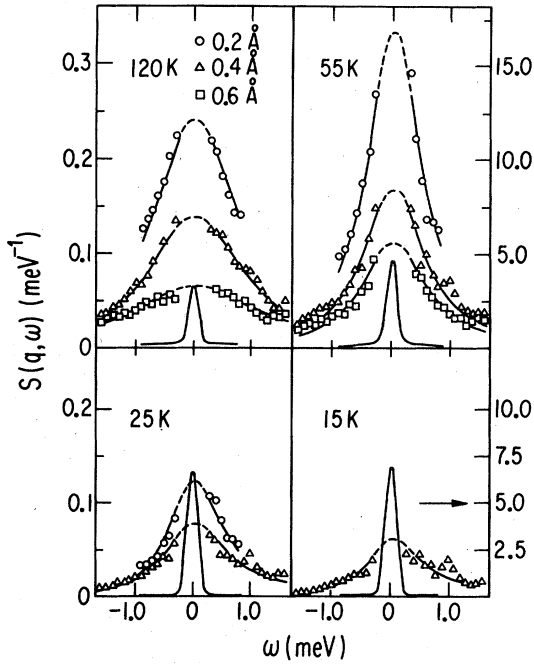


FIG. 2. Experimentally measured $S(q, \omega)$ for CuMn alloys as a function of frequency ω for several q . After Ref. 23.

It should be noted that we have assumed that $B(q, \omega)$ is essentially unaffected by the superconducting electrons except through the unknown parameter J . The indirect Rudderman-Kittel-Kasuya-Yosida (RKKY) interaction between localized (impurity) spins is expected to be altered due to the pairing of the conduction electrons which mediate it. However, Gor'kov and Rusinov⁶ have shown that this effect is not as dramatic as might have been expected because the presence of the localized spins leads to gaplessness which prevents the spin susceptibility in the superconducting state from vanishing. In the present work \bar{J} is generally taken to be a free parameter so that these effects may be viewed as implicitly included.

An alternative model for the spectral weight function in spin-glasses is the "hydrodynamical" model introduced by Dzyaloshinskii and Volovik²⁴

$$B(q, \omega) = \frac{\omega D q^2 \chi(q)}{\omega^2 + (D q^2 - \omega^2 \tau)^2} + \pi (1 - e^{-\beta \omega}) \bar{Q}(T) \delta(\omega) \quad (3.3)$$

Here D is a spin-diffusion constant and χ the static susceptibility. We have included a cutoff parameter τ in order to be able to apply sum-rule constraints which we discuss below. (In principle, this model is only valid for small ω .) As before, we will explicitly

keep track of the elastic term $(1 - e^{-\beta \omega}) \delta(\omega)$ which does not affect $B(q, \omega)$ but will enter in the equations for $u(\omega)$. There is some controversy about the coefficient of this term. It is natural to associate it with the EA order parameter since the first term in Eq. (3.3) represents the Fourier transform of

$$\bar{\chi} = [\langle \bar{S}_i(t) \cdot \bar{S}_j(0) \rangle]_c - \lim_{t \rightarrow \infty} [\langle \bar{S}_i(t) \cdot \bar{S}_j(0) \rangle]_c$$

and the second that of $\lim_{t \rightarrow \infty} [\langle \bar{S}_i(t) \cdot \bar{S}_j(0) \rangle]_c$ which is just the EA order parameter when ergodicity is assumed. Here $[\]_c$ is a configuration average. However, it has been pointed out that when the order parameter $Q(T)$ is allowed to have the presumably appropriate²⁵ low-temperature value [of $S(S+1)$] this leads to inconsistencies in the behavior of transport properties. As in Ref. 26 we will assume that $\bar{Q}(T)$ approaches S^2 as $T \rightarrow 0$, so that the elastic scattering is artificially depressed at low T . This low-temperature limit for the strength of the elastic term is the same as found in the EA model in which model these problems do not arise, and transport properties, etc., are well behaved.²⁷ In the EA case the S^2 term derives from the elastic or zz correlation function (where z is the direction along the local molecular field). Some insight into the differences of the two models may be gained by noting that in the mean-field EA model discussed above the usual ergodicity statement

$$\lim_{t \rightarrow \infty} [\langle \bar{S}_i(t) \cdot \bar{S}_i(0) \rangle]_c = [\langle \bar{S}_i \rangle \cdot \langle \bar{S}_i \rangle]_c$$

does not hold. This may be easily seen above T_c , where for the EA case the spins are entirely free, so that the left-hand side of this equation is nonzero (while the right-hand side vanishes).

We have found that for arbitrary choices of the parameters D , χ , and τ in Eq. (3.3), unphysical results may emerge in the tunneling characteristics as well as in transport properties.²⁶ Therefore, it seems essential to impose two sum rules which we now discuss.

The first of these is the standard f -sum rule²⁸

$$\int_{-\infty}^{\infty} \frac{d\omega}{\pi} \omega B(q, \omega) = \frac{\rho_s}{2\kappa} q^2, \quad (3.4)$$

where κ is the thermal conductivity and ρ_s the stiffness constant. Applying this to Eq. (3.3), we obtain

$$D\chi = \tau \rho_s / 2\kappa, \quad (3.5)$$

where we have taken $\chi(q) \equiv \chi$ independent of q for simplicity.

The second sum-rule constraint on Eq. (3.3) is derived from the definition of $S(q, \omega)$

$$\int_{\text{BZ}} d^3q \int_{-\infty}^{\infty} \frac{2}{1 - e^{-\beta \omega}} B(q, \omega) d\omega = 2\pi S(S+1) \int_{\text{BZ}} d^3q \quad (3.6)$$

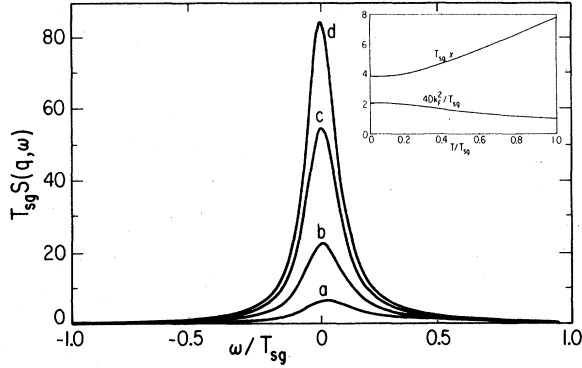


FIG. 3. Magnetic structure factor for the “hydrodynamical” model at the same set of temperatures (a–d) as in Fig. 1. Plotted in the inset are the static susceptibility and diffusion constants.

For definiteness, we took a spherical Brillouin zone (BZ) of radius $2k_F$.

With χ taken to be q independent, we may carry out the q integration analytically. The ω integration, on the other hand, is calculated numerically. [We note in passing that the EA model automatically satisfies Eq. (3.6).] In obtaining models for $B(q, \omega)$ based on Eq. (3.3) and the sum rules we assumed the following:

- (i) A small, temperature-independent value for the cutoff parameter $\tau \sim 0.1/Dk_F^2$.
- (ii) That ρ_s and κ were constant in temperature (below T_{sg}), for simplicity. Thus $D\chi = \text{const}$.
- (iii) That below T_{sg} , χ decreases monotonically with decreasing T in accord with the experimental measurements of the static susceptibility. In order for (iii) and the sum rule [Eq. (3.6)] to be satisfied, we found that a reasonable form for \tilde{Q} is $\tilde{Q} = S^2[1 - (T/T_{sg})^2]$. A further consequence of the sum rule and (iii) is that $D\chi$ falls in a narrow range for each choice of τ . For $\tau = 0.05/Dk_F^2$ we find $D\chi \sim 2k_F^{-2}$.

A plot of $S(q, \omega)$ at $q/2k_F = 0.5$, $\tau = 0.05/Dk_F^2$, and $D(T_{sg}) = 0.25T_{sg}/k_F^2$ is shown in Fig. 3, for a series of temperatures (labeled a–d) below T_{sg} . The behavior of $D(T)$ and $\chi(T)$ is shown in the inset. For this choice of parameters $T_{sg}\chi(T_{sg}) = 7.57$. Note that above T_{sg} , for χ of the form $\chi = S(S+1)/(T-\Theta)$, this implies a negative Θ corresponding to antiferromagnetic short-range order. These results may be compared with data by Murani on $CuMn$ alloys (see Fig. 2). Although the model yields very narrow widths for $S(q, \omega)$ as $q \rightarrow 0$, in the intermediate range of q values the characteristic widths are comparable to experiment. Because of the factor $q dq$ in Eq. (2.14), the small q terms are not particularly important in the superconducting density of states.

B. Numerical results and comparison with experiment

The solution to Eq. (2.14) is found numerically using an iterative procedure. The starting values of $u(\omega)$ are taken to be solutions of the AG equation

$$u(\omega) = \frac{\omega}{\Delta} + \frac{1}{\tau_s^\infty \Delta} \frac{u(\omega)}{[1 - u^2(\omega)]^{1/2}}, \quad (3.7)$$

which equation is satisfied as $T \rightarrow \infty$ by the solution of Eq. (2.14). In solving Eq. (2.14), we thus iterate down from high temperatures. Typically our program required only two or three iterations for convergences (to within 2%).

We will compare our theoretical results with tunneling data³ on a superconducting spin-glass, dilute $AgMn$. The superconductivity is induced via the proximity effect by sandwiching $AgMn$ with thick (3000-Å) Pb layers. Typical $AgMn$ thicknesses were 200 to 800 Å so that the effective Δ of the junction, for very dilute alloys, ranged from about 60% to 20% that of pure Pb . For definiteness our results are compared with those plotted in Fig. 3 of Ref. 3 for an alloy of 0.1 at. % Mn ($T_{sg} \sim 1$ K), with film thickness of 800 Å.

It is difficult to extract $N_s(\omega)$ from the measured conductance $\sigma(\omega)$ at finite T . The authors of Ref. 3 suggested an approximate scheme for estimating the temperature dependence of $N_s(0)$. We have checked their scheme by using our calculated values of $\sigma(\omega)$ to obtain $N_s(0)$ within their approximate technique and compared these to the actual values. We find the temperature variation of $N_s(0)$ given by the approach of Ref. 3 to be somewhat smaller than that obtained directly. However we will use the “thermal smearing” approach of Ref. 3 here to compare with our theoretical results for $N_s(0)$ because it is not unreasonable as a first approximation.

The alternative approach of directly comparing the computed and measured values of $\sigma(\omega)$ as a function of temperature is not feasible. This is because our calculation does not take into account the details of the proximity effect which introduce additional (“high-”) frequency variations in $N_s(\omega)$. These effects, which are amplified in the conductance at all frequencies at higher T , make it difficult to compare our theory directly with the conductance data.

In general, we have found that we cannot simultaneously fit the zero-temperature value of $N_s(0)$ and its quantitative T dependence by varying the one free parameter in our theory ζ . We believe this is because the analysis of the data, discussed above, underestimates the thermal suppression factor $[N_s(0)|_{T=T_{sg}} - N_s(0)|_{T=0}]$. A detailed study suggests that a better “unsmearing” analysis of the data would yield simultaneously agreement with both the calculated zero-temperature value of $N_s(0)$ and its T

dependence for a single value of ζ . Because the main focus of the present work is to study the T dependence of $N_s(0)$ we have chosen ζ to fit the thermal suppression factor. Therefore in plotting Ref. 3 we shifted the origin so as to yield agreement with the AG "high-temperature" limit⁵ for this value of ζ .

To make contact with previous calculations of the tunneling characteristics, it is useful to define an effective spin-flip or spin-exchange scattering time

$$\frac{1}{\tau_s^{\text{eff}} \Delta} \equiv \left[1 - \left(\frac{N_s(0)}{N(0)} \right)^2 \right]^{-1/2} \quad (3.8)$$

This form is chosen so that $1/\tau_s^{\text{eff}}$ yields the golden rule result $1/\tau_s^\infty$ which comes out naturally in the limit of noninteracting spins.⁵ In Fig. 4 we have plotted this quantity for the EA model as a function of T/T_{sg} (where T_{sg} is the spin-glass transition temperature). Our results are normalized to the "high-temperature" value τ_s^∞ , which is computed using the Abrikosov-Gor'kov theory. Also shown is a calculation of $1/\tau_s$ obtained by us previously.²² Using a golden rule calculation which includes inelastic scattering processes we found

$$\frac{1}{\tau_s} = nN(0) \frac{(J^{\text{sd}})^2}{h} \int_0^{2k_F} \frac{q dq}{2k_F^2} \times \int_{-\infty}^{\infty} n(\omega) B(q, \omega) \frac{\beta \omega}{1 - e^{-\beta \omega}} \quad (3.9)$$

where $n(\omega)$ is the Bose distribution function. A fairly typical experimental result of Schuller *et al.*,³ is plotted in Fig. 4 (dashed curve).

The curves labeled (a)–(d) correspond to different values for the parameters \bar{J}/Δ and ζ [see Eqs. (3.2) and (2.16)]. Using the value of Δ corresponding to an 800-Å AgMn film with Mn concentration of 0.1 at. % (about 20% that of pure Pb) and the Δ/\bar{J} which gives the experimentally measured spin-glass transition temperature T_{sg} in the EA model, we find (for $S = \frac{5}{2}$) that $\Delta/\bar{J} \approx 12$. Since neither T_{sg} nor Δ are accurately known in these proximity-effect systems, we have calculated our results for a range of values of Δ/\bar{J} . We illustrate the two extreme values considered, which presumably sandwich the exact one. In curve (a) we plot the results for $\Delta/\bar{J} = 12$ and $\zeta = 4$. Curve (b), for which $\Delta/\bar{J} = 0.5$ and $\zeta = 4$, is in better agreement with the experimental value (dashed line). This suggests that the actual width (in ω) of $S(q, \omega)$ is broader than that obtained using the EA model. In general we find that the curvature in $1/\tau_s^{\text{eff}}$ at low T reflects the general shape of $S(q, \omega)$ vs ω : the narrower the width (in ω) the faster the curve rises toward the high- T result. Curves (c) and (d) correspond to $S = \frac{1}{2}$. These are included for illustrative purposes only, since they yield poor agree-

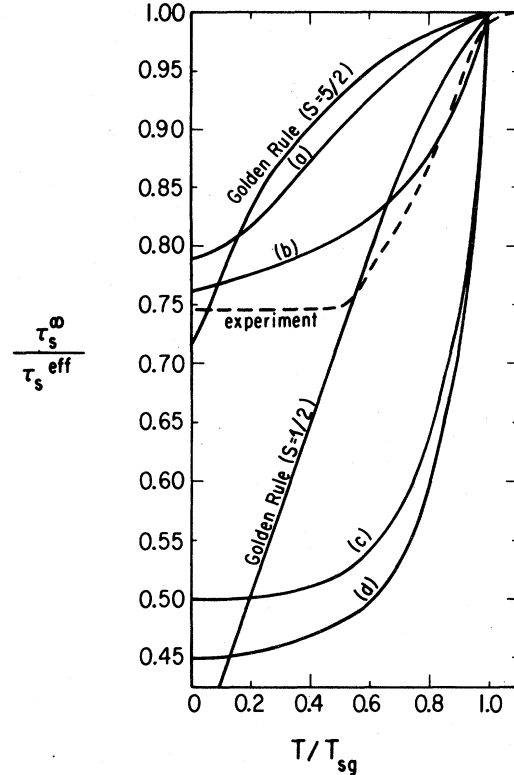


FIG. 4. Effective spin-exchange scattering time as a function of temperature in the EA theory. Curves (a) and (b) are for $S = \frac{5}{2}$ and $\zeta = 4$ with $\Delta/\bar{J} = 12$ and $\Delta/\bar{J} = 0.5$, respectively. Curves (c) and (d) are for $S = \frac{1}{2}$ and $\Delta/\bar{J} = 1$, with $\zeta = 2$ and 3 , respectively. The dashed curve is the experimental result of Ref. 3 and the golden rule calculation results are also presented.

ment with experiment. Curve (c) represents the case $\bar{J}/\Delta = 1.0$ and $\zeta = 2$ and curve (d) is for the case $\bar{J}/\Delta = 1.0$ and $\zeta = 3$. We note that the effects of varying ζ , with all other parameters including temperature fixed, are similar to those in the case of noninteracting spins. The lower ζ , the smaller is $N_s(0)$. However the thermal suppression factor $[N_s(0)|_{T=T_{\text{sg}}} - N_s(0)|_{T=0}]$, and hence the shape of the $N_s(0)$ vs T curves, is strongly affected by ζ . A plot of $\tau_s^\infty/\tau_s^{\text{eff}}$, however, does not show a strong ζ dependence. This quantity depends almost entirely on the value of the spin S . The two values of S yield rather different results. This is because the ratio of the elastic contribution (which dominates at $T=0$) and the high-temperature result go as $S^2/S(S+1)$. The suppression at low temperatures thus decreases as S increases.

As we noted in a previous paper,²² an obvious failure of the golden rule approximation is that it yields a sharp rise in $1/\tau_s$ with increasing T , whereas

the experimental results suggest that $1/\tau_s$ is nearly constant at low T . It may be seen from Fig. 4 that the more exact approach of the present work yields essentially the correct shape of $1/\tau_s^{\text{eff}}$, unlike the golden rule approximation. To understand the differences we note that in the latter approach the frequency integral is weighted by a factor $\beta\omega/(1 - e^{-\beta\omega})$, which does not appear in the self-energy calculation. This factor derives from the electron occupation factors and is characteristic of any transport-theory calculation.²⁹ It gives rise to a relatively sharp T dependence at low temperatures. Note also that the $T=0$ intercept in $\tau_s^\infty/\tau_s^{\text{eff}}$ differs in the two calculations. This follows because in the present approach there is a small contribution to the scattering from inelastic terms, which enter through the Fermi factors in Eq. (2.14). When these terms are neglected, the $T=0$ intercepts of $\tau_s^\infty/\tau_s^{\text{eff}}$ are identical in the two different approaches. While this effect is not particularly significant for the case of a highly disordered system, it will probably be important for ordered magnetic materials.

The values of $N_s(0)/N(0)$ vs T for the two $S = \frac{5}{2}$ cases (a) and (b) of Fig. 4, are plotted in Fig. 5 along with the experimental result. The general features of the experimental results are all reproduced by the theory. We note that both the "kink" [in curve (a)] in $N_s(0)$ at T_{sg} and the fact that it is temperature independent above T_{sg} are artifacts of the single-spin EA model used here, in which there is no short-range order for $T > T_{sg}$. We have generalized these results to include clusters of spins, in which case we find that the kink disappears and $N_s(0)$ is (slightly) T dependent above T_{sg} . For completeness, in the inset

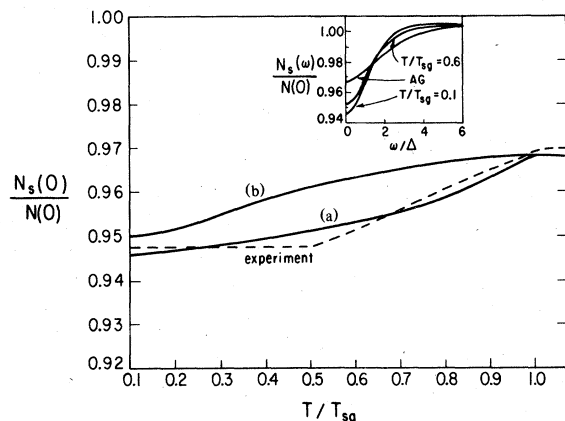


FIG. 5. Zero-frequency density of states in the EA model as a function of temperature. Curves (a) and (b) correspond to the same parameters as their counterparts in Fig. 4. The dashed curve represents the experimental result. In the inset is the ω dependence of the density of states at several temperatures. Also shown is the Abrikosov-Gor'kov (high- T) limit.

of the figure is shown the frequency dependence of $N_s(\omega)$ at several temperatures and with $\Delta/\bar{J}=0.5$ which corresponds to curve (b). Also shown is the AG (high- T) limit. In general these ω -dependent results are not in good agreement with experiment. We find that the peak height in $N_s(\omega)$ is considerably less than that observed experimentally,³ while the peak position is at higher frequencies. Since the present approach does not include any characteristics of the junction (it is more appropriate to an intrinsic magnetic superconductor), it is not surprising that the frequency dependence of $N_s(\omega)$ is in disagreement with experiment. However, it should also be noted that this general disagreement is a consequence of most theories of tunneling characteristics even in nonmagnetic superconductors when the "link" between the N and S pieces is not sufficiently weak.³⁰

In Fig. 6 are plotted the theoretical results for $N_s(0)/N(0)$ vs T for $T \leq T_{sg}$ using the hydrodynamical model discussed above. The experimental curve is indicated by the dashed line. For this model, we found that a value of $\zeta = 1.8$ fit the thermal suppression factor $[N_s(0)|_{T=T_{sg}} - N_s(0)|_{T=0}]$. This corresponds to curve (b) in the figure. To illustrate the effects of varying ζ we also plot (on a different scale) the results for $\zeta = 2.0$. It is clear that as ζ increases the thermal suppression factor decreases so that the curves become less temperature dependent. Because of sum-rule constraints (discussed in Sec. III A) we had very little freedom in choosing the other parameters in the model. Therefore, there is effectively only one fitting parameter (ζ) in this

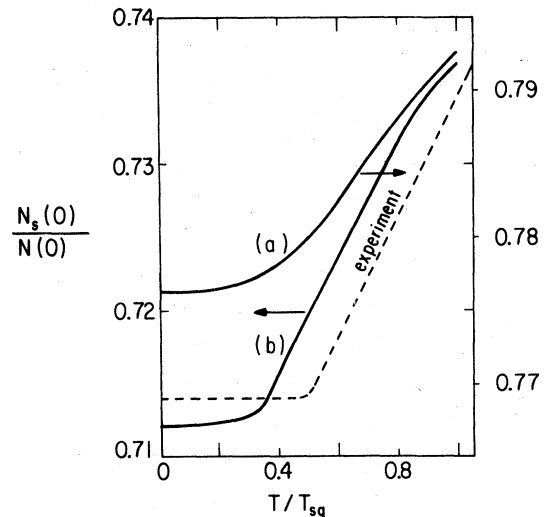


FIG. 6. Zero-frequency density of states in the "hydrodynamical" model as a function of temperature for $\Delta/T_{sg} = 3.0$ and (a) $\zeta = 2$ (right-hand scale) and (b) $\zeta = 1.8$ (left-hand scale). The parameters in $S(q, \omega)$ correspond to those plotted in Fig. 3. The dashed curve is the experimental result of Ref. 3.

theory. As dictated by experimental considerations we chose $\Delta/T_{sg} = 3$. However, our results in this model are very insensitive to Δ/T_{sg} . The values of the parameters in $S(q, \omega)$ are chosen to correspond to those shown in Fig. 3. For this case, we only considered temperatures lower than the transition temperature. This was principally due to the fact that the experimental curves are rather structureless and uninteresting above T_{sg} , so that it was not worthwhile to compute an $S(q, \omega)$ in the hydrodynamical model (which is consistent with the sum rules). It appears from the data that $N_s(0)/N(0)$ rises slowly for $T > T_{sg}$ to the limit 1.0. Since our computed curve is below this value for $T < T_{sg}$ and since it must approach 1.0 as $T \rightarrow \infty$, it follows that above as well as below the transition temperature, the present theory and experiment are in reasonably good agreement.

While not shown here, we found the general features of $N_s(\omega)$ vs ω are like those of the EA model. It is important to note that when sum-rule constraints were relaxed, we generally found non-monotonic or unphysical behavior for $N_s(0)$ vs T . This has also been observed in transport calculations using this model.²⁶ Thus we find the following correlation: models for $S(q, \omega)$ which violate the sum rules lead to unphysical results for $N_s(0)$ vs T . Similarly, if a model satisfies the sum rules we find good agreement between theory and experiment for $N_s(0)$, as shown in Fig. 6.

We have noted above that the scale of temperature variations in $N_s(0)$ can be used to learn about the characteristic energies associated with the magnetic correlations. We have also found that the derivative quantity $dN_s(\omega)/d\omega$ as a function of frequency (at low temperatures) contains similarly useful information, which it may be possible to exploit in future experiments. In particular, we find structure in the computed $dN_s(\omega)/d\omega$ near the frequency $\omega = T_{sg}$.

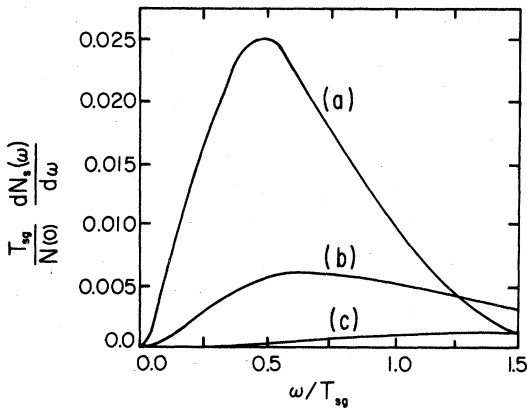


FIG. 7. $dN_s/d\omega$ vs ω for (a) $T/T_{sg} = 0.1$, (b) $T/T_{sg} = 0.5$, and (c) for the AG ($T \rightarrow \infty$) limit. These curves are computed for the EA model with $\Delta/\bar{J} = 12$ and $\zeta = 3$.

This behavior, which is reminiscent of what is observed in strong-coupling superconductors⁴ is illustrated in Fig. 7 for the EA model with the parameters $\zeta = 4$ and $\Delta/\bar{J} = 12$. Very similar results are obtained for the hydrodynamical model. In both cases a peak was obtained at a frequency ω somewhat less than T_{sg} ; its behavior was rather insensitive to the choice of all the parameters in the two models. The peak height decreased and the frequency of the maximum increased with increasing T . For comparison, predictions of the AG theory (high T) are also plotted in the figure. Note that the AG theory yields a featureless curve in this region of frequency.

This structure in $dN_s/d\omega$ may have been seen in an induced spin-glass superconductor.³⁰ However, quantitative comparison with the data is not possible since the behavior of $N_s(\omega)$ is strongly affected by the proximity-effect sandwich. Future measurements on intrinsic magnetic superconductors should be analyzed in this manner. Since we have found that these derivative analyses contain direct information about the magnitude of the magnetic ordering temperature, such measurements may prove a useful way to determine whether coexistence has, in fact, occurred.

IV. CONCLUSIONS

While there has been an extensive amount of literature devoted to computing the phase diagram for magnetic and superconducting order, considerably less attention has been paid to the behavior of the density of states $N_s(\omega)$ in magnetic superconductors. In principle, superconducting tunneling experiments [which measure $N_s(\omega)$] yield valuable information about the interplay between magnetism and superconductivity. They can be exploited not only to obtain a parameterization of the spin-flip lifetime τ_s (which, in part, determines the phase diagram for coexistence), but more importantly to gain information about the magnetic structure factor $S(q, \omega)$, averaged over q .

In the present work we demonstrated how to interpret the temperature-dependent behavior of the zero-frequency tunneling state density in induced superconducting spin-glasses. Presumably for intrinsic magnetic superconductors an analysis of the finite frequency behavior will also be informative. We found that the scale of temperature variations in $N_s(0)$ reflects the characteristic width (in ω space) of the magnetic structure factor. While a golden rule calculation is adequate for estimating the magnitude, at all temperatures of

$$1/\tau_s^{\text{eff}} \Delta = \{1 - [N_s(0)/N(0)]^2\}^{-1/2}$$

it reproduces the shape of this function of temperature rather poorly. Thus, from the point of view of

learning in detail about $S(q, \omega)$ the full dynamical Eliashberg-like equation for $N_s(\omega)$ must be solved, as was done here. We view the success of the present theory in explaining the tunneling data as a confirmation of the correctness of the many-body Eliashberg-like equation for the superconducting density of states.

Several other interesting observations should be noted.

(i) Models for $S(q, \omega)$ which violated sum rules consistently yielded poor agreement between theory and experiment, whereas those that satisfied them led to good agreement.

(ii) There is always (even at $T=0$) a finite contribution to the spin-exchange lifetime from inelastic processes. This term, which does not appear in the golden rule calculation, thus, makes coexistence of magnetism and superconductivity less likely than might be expected, based on a golden rule calculation of $1/\tau_s^{\text{eff}}$.

(iii) It appears that tunneling measurements may be useful in ascertaining whether magnetic order exists in a superconductor. This is useful, particularly in superconducting spin-glasses when it may be difficult³¹ to prove coexistence.

(iv) Finally, we predict the existence of a peak in $dN_s/d\omega$ at $\omega \sim T_{\text{sg}}$. This peak height decreases with increasing temperature and is essentially zero at a temperature $T > T_{\text{sg}}$.

ACKNOWLEDGMENTS

We thank I. Schuller and P. Chaikin for helpful discussions of their data. K. L. acknowledges a grant from the Alfred P. Sloan Foundation. This work was supported in part by the NSF Materials Research Laboratory, Grants No. DMR 77-23798 and No. DMR 77-12637.

- ¹O. Fischer, A. Treyvand, R. Chevrel, and M. Sergent, *Solid State Commun.* **17**, 721 (1975); R. N. Shelton, R. W. McCallum, and H. Adrian, *Phys. Lett. A* **56**, 213 (1976).
- ²B. T. Matthias, E. Corenzwit, J. M. Vandenberg, and H. E. Borz, *Proc. Natl. Acad. Sci. U.S.A.* **74**, 1334 (1977).
- ³I. Schuller, R. Orbach, and P. M. Chaikin, *Phys. Rev. Lett.* **41**, 1413 (1978).
- ⁴W. L. McMillan and J. M. Rowell, in *Superconductivity*, edited by R. D. Parks (Marcel Dekker, New York, 1969).
- ⁵A. A. Abrikosov and L. P. Gor'kov, *Zh. Eksp. Teor. Fiz.* **39**, 1781 (1961) [*Sov. Phys. JETP* **12**, 1243 (1961)].
- ⁶P. Gor'kov and A. I. Rusinov, *Sov. Phys. JETP* **19**, 922 (1964).
- ⁷J. Keller and R. Benda, *J. Low Temp. Phys.* **2**, 141 (1970).
- ⁸T. Lee, Y. Izyumov, and J. L. Birman, *Phys. Rev. B* **20**, 4494 (1979).
- ⁹H. Suhl, *J. Less-Common Met.* **62**, 225 (1978).
- ¹⁰S. Maekawa and M. Tachiki, *Phys. Rev. B* **18**, 4688 (1978).
- ¹¹M. V. Sadovskii and Yu. N. Skryabin, *Phys. Status Solidi* **94**, 1 (1979). The authors compute the spin-flip scattering rate for a superconducting spin-glass. However, they find it to be temperature independent, in contrast with the present paper and the experimental results.
- ¹²P. Entel and W. Klose, *J. Low Temp. Phys.* **17**, 529 (1974).
- ¹³C. Balseiro and L. M. Falicov, *Phys. Rev. B* **19**, 2548 (1979).
- ¹⁴K. H. Bennemann and S. Nakajima, *Phys. Rev. Lett.* **16**, 243 (1966).
- ¹⁵N. F. Berk and J. R. Schrieffer, *Phys. Rev. Lett.* **17**, 433 (1966). See for example, A. Toxen, P. C. Kwok, and R. J. Gambino, *Phys. Rev. Lett.* **21**, 792 (1968).
- ¹⁷A. B. Kaiser and M. J. Zuckermann, *Phys. Rev. B* **1**, 229 (1970).
- ¹⁸W. L. McMillan, *Phys. Rev.* **175**, 559 (1968).
- ¹⁹M. J. Nass, K. Levin, and G. S. Grest (unpublished).
- ²⁰D. J. Scalapino, J. R. Schrieffer, and J. W. Wilkins, *Phys. Rev.* **148**, 263 (1966).
- ²¹S. F. Edwards and P. W. Anderson, *J. Phys. F* **5**, 965 (1975).
- ²²G. S. Grest, K. Levin, and M. J. Nass, *Phys. Rev. B* **21**, 1219 (1980).
- ²³A. P. Murani and J. L. Tholence, *Solid State Commun.* **22**, 25 (1977).
- ²⁴I. E. Dzyaloshinskii and G. E. Volovik, *J. Phys. (Paris)* **39**, 693 (1978).
- ²⁵Since $\chi = [\langle S^2 \rangle - \langle S \rangle^2]_c / T = [S(S+1) - Q] / T$, it follows that $Q \rightarrow S(S+1)$ as $T \rightarrow 0$ in order for the susceptibility to be finite at zero temperature.
- ²⁶K. H. Fischer, *Z. Phys. B* **34**, 45 (1979).
- ²⁷K. Levin, C. M. Soukoulis, and G. S. Grest, *J. Appl. Phys.* **50**, 1695 (1979).
- ²⁸D. Forster, *Hydrodynamic Fluctuations, Broken Symmetries and Correlation Functions* (Benjamin, Reading, Mass., 1975).
- ²⁹M. P. Greene and W. Kohn, *Phys. Rev.* **137**, A513 (1965).
- ³⁰P. M. Chaikin and I. Schuller (private communication).
- ³¹D. Davidov, K. Baberschke, J. Mydosh, and G. Nieuwenhuys, *J. Phys. F* **7**, L47 (1977).